Hindawi
Journal of Clinical Pharmacy and Therapeutics
Volume 2023, Article ID 9955105, 12 pages
https://doi.org/10.1155/2023/9955105

Research Article

In Silico Screening, In Vitro M^{pro} Inhibitory, and Adjunctive Therapy Value of Minocycline for the Treatment of COVID-19

Yaru Han,[1] Xianxiang Bai,[1] Si Wu,[1] Xiurong Luan,[1] Liwen Ren,[2] Jinhua Wang,[2] Zhanfei She,[1] Bin Xiao ,[1] and Guanhua Du [2]

[1]*General Clinical Research Center, Ordos Central Hospital, Ordos School of Clinical Medicine, Inner Mongolia Medical University, Ordos 017000, China*
[2]*Beijing Key Laboratory of Drug Target Identification and Drug Screen, Institute of Materia Medica, Chinese Academy of Medical Sciences & Peking Union Medical College, Beijing 100050, China*

Correspondence should be addressed to Bin Xiao; michael-bin@163.com and Guanhua Du; dugh@imm.ac.cn

Received 19 October 2022; Revised 25 August 2023; Accepted 22 September 2023; Published 9 October 2023

Academic Editor: Samuel Silvestre

What Is Known and Objective. Novel coronavirus disease (COVID-19) is still ravaging globally since its first discovery in 2019. With the continuous emergence of severe acute respiratory syndrome-coronavirus-2 (SARS-CoV-2) mutant strains, therapeutic entities are still needed to be discovered. This study was to explore SARS-CoV-2 inhibitors and therapeutic entities for COVID-19. *Methods*. Based on Lipinski's rule of 5, a small-scale "old" drug database (clinical drugs being used in Ordos Central Hospital) was established, and in silico screening of M^{pro} inhibitors was conducted. Binding affinity and interaction as well as structure-affinity relationship were analyzed. Furthermore, molecular dynamic (MD) simulation of the selected drugs was performed to understand the conformational changes in docked complex. In vitro M^{pro} inhibition tests were performed according to established methods. Finally, literature review of potential "old" drug for the treatment of COVID-19 was conducted. *Results and Discussion*. The antibiotic minocycline, an inhibitor of bacterial ribosomal RNA, was screened out which showed the highest binding affinity (−9.6 kcal/mol). Beside the hydrogen bond with Cys145 and hydrophobic interactions, minocycline formed a pi-cation with His41, which strongly supported minocycline as a Michael addition acceptor to bind with the catalytic site of M^{pro}. MD simulation results show that minocycline displayed less conformational changes. The structure-affinity relationship was summarized based on minocycline analogs, and minocycline showed in vitro M^{pro} inhibitory activity with IC_{50} of 5 mM. More importantly, the literature review found that minocycline had both in vitro and in vivo broad-spectrum antiviral as well as anti-inflammatory activities, and the levels of a broad spectrum of biological markers during minocycline administration were opposed to those of COVID-19 conditions (both severe and nonsevere). *What is New and Conclusion*. Minocycline deserves an adjunctive therapeutic option for COVID-19 condition (both severe and nonsevere). This study shed a new light on drug-repurposing strategy for the viral disease.

1. What Is Known and Objective

Until now, globally ongoing epidemic of the novel coronavirus (severe acute respiratory syndrome-coronavirus-2, SARS-CoV-2) disease (COVID-19) has infected more than 765,000,000 people and killed more than 6,900,000 patients according to the World Health Organization (WHO). Common symptoms of COVID-19 include fever, cough, shortness of breath, and dyspnea. In more severe cases, infection causes pneumonia, severe acute respiratory syndrome, kidney failure, or even death [1]. Although the vaccinated population in the world has exceeded 13,344,000,000 to end this catastrophic epidemic, more treatments other than vaccines need to be developed [2]. Remdesivir is the only drug approved by the Food and Drug Administration (FDA) for the treatment of COVID-19. Ritonavir-enhanced nirmatrelvir (Paxlovid), molnupiravir, and certain anti-SARS-CoV-2 monoclonal antibodies (MABs) have received emergency use authorizations from the FDA for the treatment of COVID-19. Antiviral therapies

are being investigated for the treatment of COVID-19, and the drugs prevent viral replication through various mechanisms, including blocking SARS-CoV-2 3-chymotrypsin-like protease (3CLpro, also named as M^{pro}) and RNA-dependent RNA polymerase (RdRp), causing viral mutations. Besides, the previous study found that the combination of brequinar (BRQ), a dihydroorotate dehydrogenase (DHODH) inhibitor, and dipyridamole (DPY), a remedial pathway inhibitor, expresses a strong synergistic antiviral activity to treat SARS-CoV-2 [3]. As SARS-CoV-2 mutant strains continue to emerge, new therapeutic entities are still needed to be discovered.

Nonstructural proteins (NSPs) are involved in SARS-CoV-2 RNA transcription and translation, protein synthesis, protein processing and modification, virus replication, and host infection [4]. In NSPs, M^{pro} is automatically cleaved from polyproteins to produce mature enzymes and further cleaves downstream NSPs at 11 sites to release NSP 4–16 [5]. The structure and catalytic mechanism of SARS-CoV M^{pro} allows it as a promising target for anti-coronavirus drug development. To develop an anti-SARS-CoV-2 drug from scratch is theoretically time consuming [6]. We can test existing broad-spectrum antivirals for their metabolism, used dosages, efficacy, and side effects. However, the side effects of broad-spectrum antivirals should not be underestimated [7]. Because "old drugs" have been prepared, the medication has sufficient experience, and the safety and pharmacokinetic parameters are well known, screening for SARS-CoV-2 therapeutic candidates from existing clinical "old drugs" is always a good strategy [8, 9]. From this strategy, Masitinib was recently discovered as a broad coronavirus 3CL inhibitor that blocked SARS-CoV-2 virus replication [10].

In this study, we established a small-scale "old drug" database (clinical drugs being used in Ordos Central Hospital) according to *Lipinski*'s rule of 5 and conducted in silico screening of M^{pro} inhibitors by molecular docking. Binding affinity and interaction as well as structure-affinity relationship were analyzed to better understand the potentiality. The in vitro M^{pro} inhibition test was conducted based on established methods. Finally, literature support for the potentiality of anti-SARS-CoV-2 and treatment of COVID-19 was reviewed and analyzed. This study will provide contribution to the transient ongoing infectious diseases.

2. Methods

2.1. Pharmacophore Study of the Co-Crystal Ligand N3. The crystal structure of SARS-CoV-2 M^{pro} in complex with designed ligand N3 (2.1 Å resolution, PDB code: 6LU7) was determined by Professors Zihe Rao and Haitao Yang's research team from Shanghai Tech University [11]. The protein coordinates of the M^{pro} used in this study were donated by Zihe Rao et al. in Jan 28th, 2020. Based on the structure, key helixes/loops, amino acid residues, and hydrophobic interactions in the binding site were investigated. The pharmacophore of N3 was summarized and was used as a control in the following in silico study.

2.2. Drug Database Establishment. According to *Lipinski*'s RULE of 5, we established a small-scale database including 135 drugs clinically being used in Ordos Central Hospital [12]. Requirement-reached drug 2D structures were drawn by ChemDraw Professional 17.0 software (CambridgeSoft Corporation, Cambridge, MA, USA). The 2D structures of candidates were converted into 3D structural data by Chem3D ultra 17.0 software (CambridgeSoft Corporation, Cambridge, MA, USA), and all structures of the ligands were energy-minimized.

2.3. Molecular Docking by AutoDock Vina. We applied a workflow for molecular docking which was described in our previous work [13–15]. The chain B (co-crystal ligand N3 in 6LU7) and chain C (water molecules) were deleted, and chain A was prepared for docking within the molecular modeling software package Chimera 1.10.2 (National Institutes of Health, Bethesda, MD, USA) [16]. Adding polar hydrogens and Kollman charges, Gasteiger computing and grid box parameters defining were done using MGL tools 1.5.6 (The Scripps Research Institute, La Jolla, CA, USA) [17, 18].

All the ligands were set as flexible, and the receptor was set as rigid. Docking calculations were performed using AutoDock Vina 1.1.2 software (The Scripps Research Institute, La Jolla, CA, USA) [19]. A search grid box was set to cover the whole surface of M^{pro} protein to collect all possible orientations and conformations of the ligand paired with the protein (including compounds outside the active site). For which, the center was set as center_$x = -23.982$, center_$y = 12.114$, center_$z = 57.466$, and the size was set as size_$x = 58$, size_$y = 78$, size_$z = 66$. Spacing angstrom was set as 1.000, and the exhaustiveness was set as 100. The default settings and the AutoDock Vina scoring function were applied.

Totally, 9 binding modes were generated by AutoDock Vina for each compound, and the mode (even outside the active site) with the highest binding affinity was selected as the most predictable. Visual investigation and analysis of ligand-protein interactions were performed using PyMOL V.1.5 (Schrodinger LLC, New York, NY, USA).

2.4. Re-Docking by Discovery Studio. The 3D protein structure of M^{pro} was defined as the receptor and optimized by hydrogenation, dehydration, and removing redundant residues. Location of N3 in the cocrystal was defined as the active site with a radius as 13.890841 covering the binding region. The X, Y, and Z centers were set as −10.797, 12.536, and 68.905, respectively. Molecular structures of ligands were prepared and converted to 3D structures. The molecular docking was performed using CDOCKER tool. -CDOCKER_ENERGY and -CDOCKER_INTERACTION_ENERGY were used to score the interaction between the receptor and ligand. Discovery Studio (DS) 2022 software (BIOVIA, San Diego, CA, USA) was used for the docking, visualization, and analysis [20].

2.5. Molecular Dynamics (MD) Simulation. MD approach is widely used to assess atoms' behavior, structural stability, and study the conformational changes on atomic level. Herein, after the molecular docking, MD simulation was performed on the compounds with best affinity by DS. The complexes were minimized using the CHARMM force field. During the solvation process, default waterbox size options were selected, and the waterbox size was adjusted to match the protein's size using a rectangular waterbox type with an edge distance of 7.0 Å. To neutralize the system and to achieve a NaCl concentration of 0.145 M, 20 Na^+ ions and 17 Cl^- ions were added to the complex. A total of 3,000 steps of energy minimization were performed using the steepest descent method. Subsequently, the minimized system was equilibrated and run for 20 ps at a constant temperature of 300.00 K, followed by a 10 ns production run. Basic parameters for trajectory analysis such as root mean square deviation (RMSD), root mean square fluctuation (RMSF), and hydrogen bond (H-bond) interactions were analyzed for each protein-ligand complex.

2.6. Structure-Affinity Relationship Study. Considering the generated information is relatively limited, investigation of the promising drug analogs will provide information for further study such as structure modification. After the in silico screening and the re-docking study, the analogs of the promising drug were collected by referring to literatures from PubMed, Elsevier, Springer, and Google Scholar. Then, one-by-one docking of the analogs targeting on M^{pro} was performed. Based on the analogs' binding affinities, the structure-affinity relationship of the promising drug was summarized.

2.7. In Vitro Activity Assays of the SARS-CoV-2 M^{pro} Inhibitors. The inhibition rate of "old drug" on M^{pro} enzyme was measured using the 2019-nCoV M^{pro} inhibitor screening kit (P0312S, Beyotime Biotechnology, Shanghai, China) according to the manufacturer's instructions. This kit was monitored at excitation of 340 nm and emission of 490 nm wavelengths on a microplate multimode reader by fluorescence resonance energy transfer. The percentage inhibition was calculated.

2.8. Literature Review of Promising Drug. After the in silico and in vitro study, we further questioned whether the promising "old drug" possessed documented biological activities associated with the pathological changes in COVID-19 condition. We searched PubMed, Elsevier, Springer, and Google Scholar for articles describing SARS-CoV-2 virus, COVID-19 condition, and the biological changes during the drug use. The condition of COVID-19 and the drug effect on pathological changes were summarized.

3. Results and Discussion

3.1. Pharmacophore of the Co-Crystal Ligand N3. As illustrated in Figure 1, M^{pro} monomer has three domains: domain I (6 antiparallel β-sheet), domain II (6 antiparallel β-sheet), and domain III (α-helixes, closely related to proteolytic activity), and a long loop connects domains II and III. A highly conserved substrate-binding pocket (with a Cys145-His41 catalytic dyad) is located in a cleft between domains I and II, suggesting the antiviral inhibitors targeting this site should have a broad-spectrum anti-coronavirus activity [11].

As shown in Figure 1, a covalent bond between the Sγ atom of Cys145 and the Cβ of the vinyl group is formed, supporting the critical Michael addition in the catalytic mechanism [5]. The lactam of P1 site inserts into the subsite S1 and forms a hydrogen bond with His163, while Leu of P2 site inserts deeply into a hydrophobic subsite. The Val of P3 site is exposed to solvent, tolerating a variety of functional group substitutions. The Ala of P4 is in a hydrophobic pocket. P5 site makes van der Waals interactions with Pro168, Thr190, and Ala191, while the aromatic ring forms van der Waals contacts with Thr24 and Thr25. N3 forms multiple hydrogen bonds with the active site residues, locking the inhibitor inside the binding pocket, which determines the inhibition of the enzyme as well as the coronavirus replication [11].

M^{pro}, which is highly conserved among all coronavirus, is a good target for the development of a single antiviral agent or in combination with other potential therapies to provide an effective first line of defense against all coronavirus-associated diseases [16]. The cocrystal structure of SARS-CoV-2 M^{pro} complexed with N3 is a good model for identifying inhibitor lead through in silico screening.

3.2. In Silico Screening by AutoDock Vina. For docking validation, N3 was re-docked into M^{pro}. The described docking workflow allowed top-ranked and reproduced binding conformation which was close to those of the 6LU7 co-crystal structure (checked by PyMOL, RMSD of 1.126 Å). In this study, a molecule with binding affinity ≤ -8.5 kcal/mol was treated to be potential based on recent reports on in silico screening of SARS-CoV-2 M^{pro} inhibitors [21].

All the 135 "old" drug structures, biological activities, targets, and top-ranked binding affinities were summarized (Supporting Information Table. S1). In which, 6 molecules including anti-HIV drug (raltegravir), antibacterial drugs (cefonicid, cefoperazone, and minocycline), and antidiabetic drugs (canaglifozin and glyburide) showed high affinities (≤ -8.5 kcal/mol) as well as interesting binding conformations (bound to the M^{pro} active site and formed interesting interactions with key residues). In particular, the antibiotic minocycline, an inhibitor of bacterial ribosomal RNA, showed the highest binding affinity (−9.6 kcal/mol) compared to N3 (−7.7 kcal/mol). These small molecular drugs might be M^{pro} inhibitors of SARS-CoV-2.

Minocycline is a second-generation tetracycline antibiotic with an established safety profile that has been used in clinic for more than 30 years. It selectively binds to the 16S rRNA, inhibiting the binding of RNA to ribosomes, and interferes with protein synthesis [22]. The main treatment conditions of minocycline were Gram-positive/negative bacterial infections and the more recent multidrug-resistant *Acinetobacter baumannii* [23].

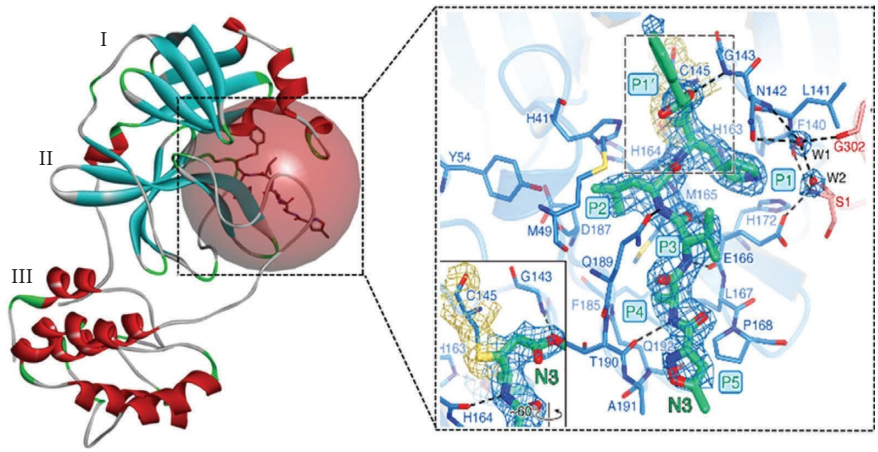

FIGURE 1: N3 bound in M^{pro} active site and the diagram of the interactions in the coco-crystal [11]. P1, P1′, P2, P3, P4, and P5 sites of N3 are indicated; 2Fo-Fc density map is shown around N3 molecule in blue mesh, C145-A in yellow mesh, and water in blue mesh. The key residue is shown in stick, hydrogen bond is shown in black dashed line, and water is shown as red sphere.

3.3. Re-Docking of N3 and Minocycline by Discovery Studio. To further validate the docking result, re-docking and comparison of docking results generated by different software are academically consensus. From the CDOCKER results generated by Discovery Studio, N3 (Figure 2(a)) formed conventional hydrogen bonds with residues Phe140, His163, His164, Glu166, Gln189, and Thr190. The isoxazole group formed pi-alkyl interaction with Ala191 and Pro168. The aromatic ring formed van der Waals' forces with residues Thr24, Thr25, Leu27, and Cys145. In addition, N3 molecule forms covalent bonds with multiple residues of M^{pro}. The docking results were closely consistent with the co-crystal structure (checked by PyMOL, RMSD of 1.650 Å).

For minocycline (Figure 2(b)), it contains multiple hydrophilic groups which formed conventional hydrogen bonding networks with key residues Phe140, Gly143, Cys145, His164, and Glu166 in the active site. The hydrophobic aromatic rings formed van der Waals' forces with multiple amino acid residues of M^{pro}. It is commonly accepted that the covalent bond formed between the Cys145-His41 catalytic dyad and the designed compound would increase the M^{pro} inhibition potency, resembling the intermediate during substrate cleavage [5]. Beside the hydrogen bond between Cys145 and 2-carboxamide, a critical pi-cation formed between His41 and 4-dimethylamino group, which strongly supported minocycline as a Michael addition acceptor binding with the exact catalytic site to inhibit M^{pro}. These results indicated that the multiple especially critical interactions stabilized minocycline-M^{pro} in a low energy state, which was required for M^{pro} selection and antiviral activities.

3.4. MD Simulation. The ligand-binding status in the physiological milieu was predicted by MD simulation. The MD simulation of M^{pro}-N3 and M^{pro}-minocycline complexes was performed for 10 ns. RMSD is calculated considering the proteins' backbone with respect to the initial conformations [24]. The RMSD values of the M^{pro}-N3 complex remained constant (~3 Å) from 0–4 ns and reached another plateau state after 5 ns and maintained the deviation below 2.5 Å. The RMSD value of M^{pro}-minocycline complex was found to be stable without significant deviation which was maintained below 3.5 Å (Figure 3(a)). These results preliminarily showed that there was no major deviation or conformation adjustment as the interaction of these ligands with the protein is stable. The RMSF was used for quantifying local changes/amino acid fluctuations along the protein chain [25]. Fluctuations for each of the individual amino acid of the target protein in case of N3 and minocycline were observed from the RMSF values. The average fluctuation of the amino acid residue for M^{pro}-N3 complex was 5.26 Å, and that was 6.85 Å for the M^{pro}-minocycline complex (Figure 3(b)). Less RMSF fluctuation indicates more interaction with the active site [26]. Subsequently, we investigated the persistence and variability of H-bond interactions by plotting H-bond thermograms. As shown in Figure 4, the H-bond interactions changed dynamically at different times throughout the simulation, but the total number of the interactions remained relatively stable. This indicated that the H-bond interactions in the M^{pro}-minocycline complex were highly persistent and stable.

3.5. Structure-Affinity Relationship of Minocycline. By referring to the literatures from PubMed, Elsevier, Springer, and Google Scholar, a database of minocycline analogs (44-compound, in which 21 compounds were clinical drugs) was established. After molecular docking, the chemical structures and top-ranked binding affinities of the analogs were summarized (Supporting Information Table. S2).

Indeed, minocycline showed a promising highest binding affinity among all the 44 analogs. Structures containing the main octahydrotetracene-2-carboxamide skeleton were analyzed and the structure-affinity relationship was summarized (Figure 5). Carbonyl functional groups should be kept, and the middle hydroxyl group might be better if changed to carbonyl. Furthermore, the terminal 2-carboxamide could be modified with moderate (not too long) moiety. On the 4,7-bis(dimethylamino) side,

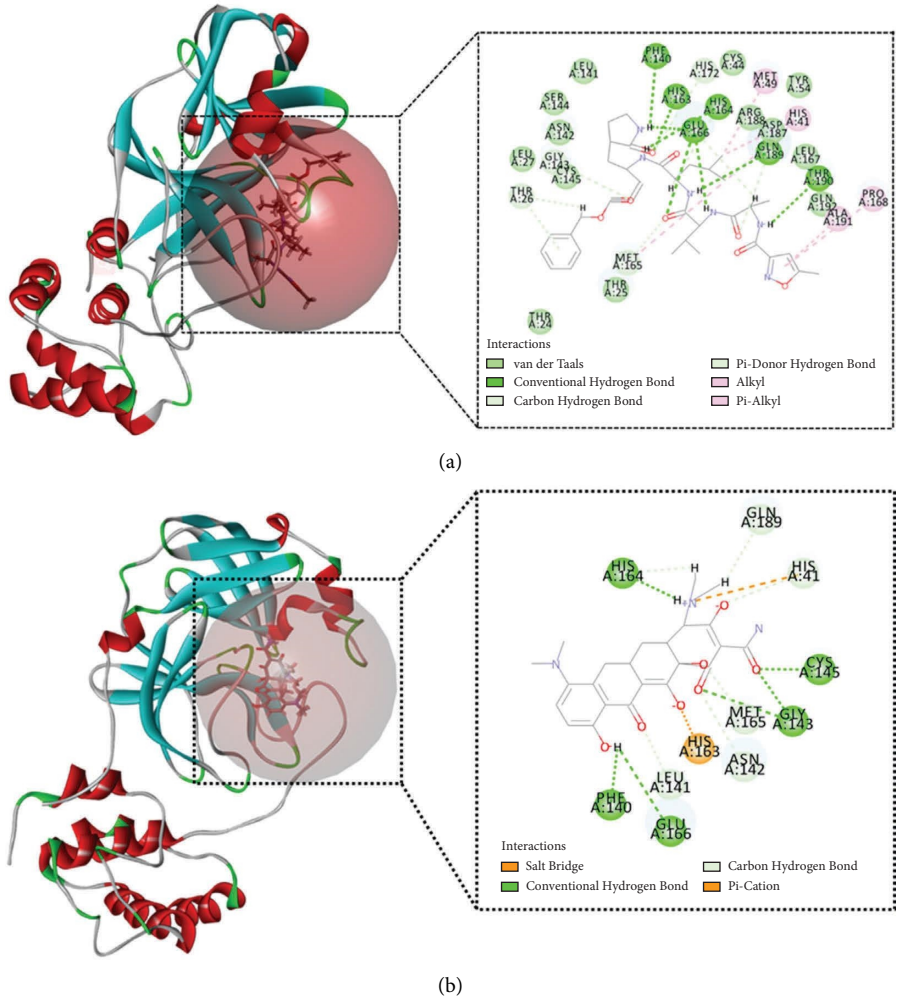

FIGURE 2: (a) Diagram of the interactions between N3 and M^{pro} and (b) diagram of the interactions between minocycline and M^{pro}. The key amino acid residue is shown in sphere, salt-bridge is shown in orange dashed line, conventional hydrogen bond is shown in green dashed line, carbon-hydrogen bond is shown in light blue dashed line, and pi-cation is shown in bright-orange dashed line.

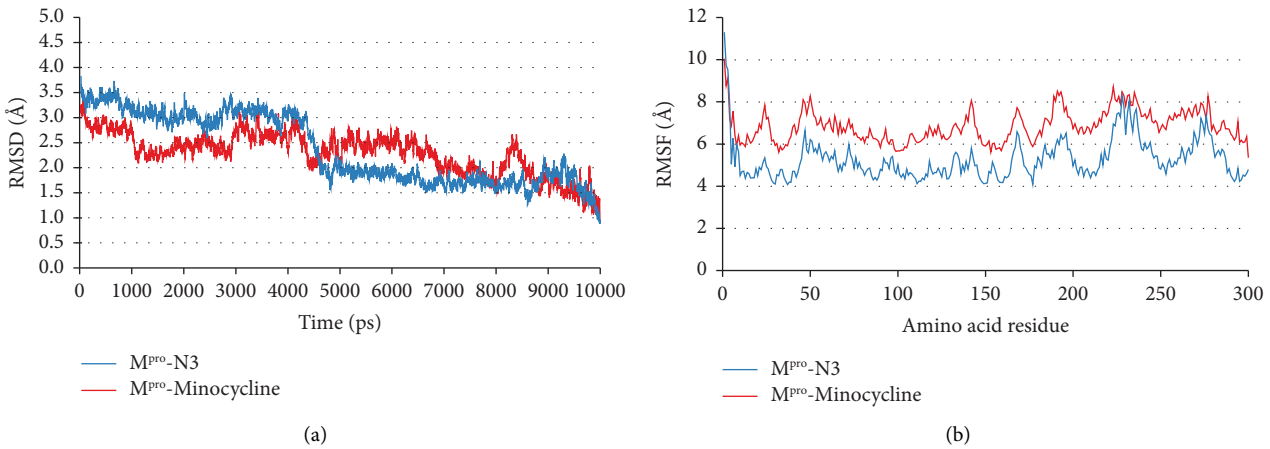

FIGURE 3: Different stability-related parameters of docked complexes using M^{pro} obtained from MD analysis: (a) RMSD and (b) RMSF.

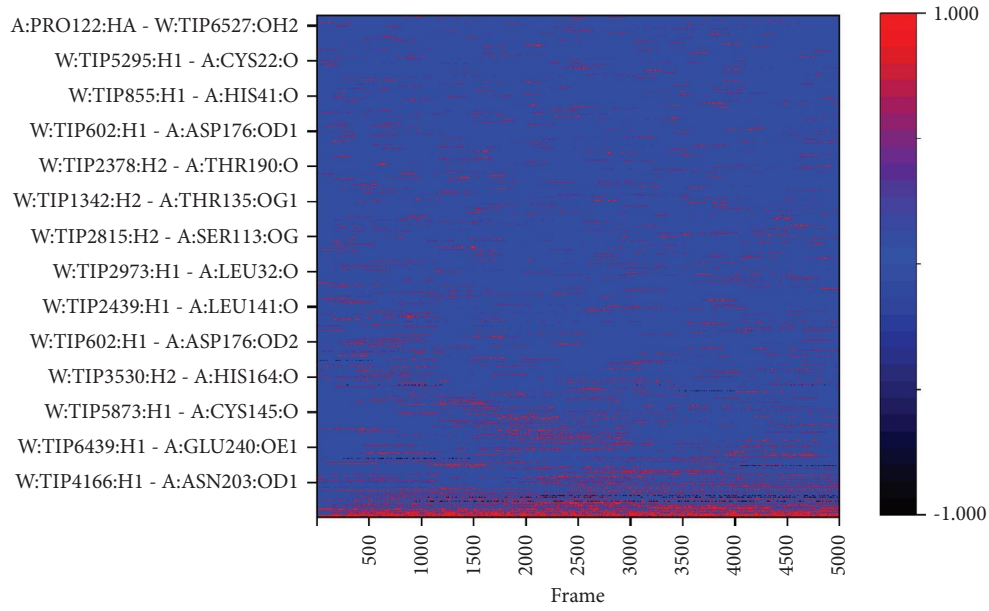

Figure 4: H-bond interaction heatmap for 0–5000 frames (0–10 ns).

4-dimethylamino group is critical for the high affinity, and the *S*-stereochemistry of C4 is better than the *R*-stereochemistry, which was also verified from the previous binding mode investigation that it could form the key covalent bond with His41.

Docking simulation and the structure-affinity relationship study revealed that critical covalent bond formed between minocycline and the Cys145-His41 catalytic dyad of M^{pro}, which helped us to better understand why the functional groups as well as the tetracycline skeleton could be suitable for the M^{pro} active site binding.

3.6. In Vitro Activity Assays of the SARS-CoV-2 M^{pro} Inhibition. As shown in Figure 6, minocycline showed M^{pro} inhibitory activity in a dose-dependent manner with IC_{50} of 5 mM. The in vitro validation result suggests that the inhibitory activity against SARS-CoV-2 M^{pro} of minocycline might be beneficial in addition to other well-known mechanisms. Furthermore, minocycline could be used as an interesting lead to design analogs that can more potently and selectively inhibit SARS-CoV-2 M^{pro} to improve its antiviral activity and avoid the unwanted adverse effects associated with other mechanisms.

Minocycline has been used in pharmacological conditions of both bacterial and mycoplasma infections. Moreover, minocycline appears to have broad-spectrum antiviral activities: reducing West Nile virus titers in brain-derived cell types, reducing Japanese encephalitis-induced damage in neuronal cells, inhibiting H7N9 replication in human lung epithelial cells, and attenuating pathogenic immune responses during infection with human and simian immunodeficiency virus (HIV/SIV) [27–31]. Based on molecular docking and dynamic studies, minocycline was proposed as potential antiviral therapy against Congo Crimean hemorrhagic fever virus to inhibit the binding of virus to host nucleoprotein [32].

In a randomized controlled trial of dengue hemorrhagic fever patients, compared with standard-of-care, combination therapy with doxycycline (analog of minocycline) significantly decreased the TNF and IL-6 levels and mortality [33]. Tetracycline inhibiting proinflammatory cytokines and matrix metalloproteinases plays a key role in coronavirus acute infection and is involved in chemokine activation and in tissue destruction [34, 35]. Of note, this immunomodulatory effect seems to be dsRNA-mediated [36].

3.7. Literature Review of Minocycline. From PubMed, Elsevier, Springer, and Google Scholar databases, articles describing COVID-19 and minocycline use until 2022, June 1st, were searched. More than 10,000 papers including published and preprints were found, in which 1430 papers clearly clarified the biochemical indexes of COVID-19 patients, and 706 papers were associated with the anti-inflammatory effect of minocycline. The effect of COVID-19 conditions and minocycline on selected biomarkers including erythrocyte sedimentation rate (ESR), C-reactive protein (CRP), lactose dehydrogenase (LD), D-dimer, CD^{4+}T cell, CD^{8+}T cell, tumor necrosis factor (TNF)-α, interferon (IFN)-γ, interleukin (IL)-6, and IL-10 were summarized and analyzed (Table 1).

A variety of clinical data revealed that the inflammatory factor storm (IFS) existed and played a critical role in severe or fast-progressive COVID-19 condition. In the later phase, the level of ESR, CRP, IL-6, and D-dimer increased and the counts of lymphocytes, total T cells, CD^{4+}T cells, and CD^{8+}T cells were dramatically reduced, while patients in declining period presenting decreased levels of TNF-α, IFN-γ, IL-6, and IL-10 and restored counts of T cell [21, 63, 64, 85]. In severe COVID-19 patients, the elevation of the CRP level and white blood cell count might be accompanying with bacterial infection, and antibiotics were usually prescribed [49]. As shown in Table 1, the levels of

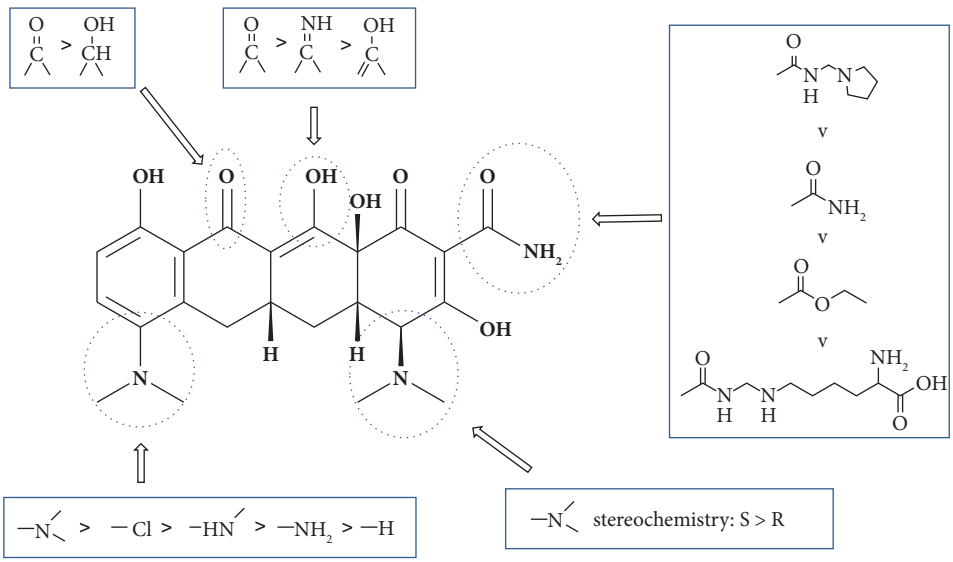

Figure 5: Primary structure-affinity relationship illustration of minocycline targeting on M^{pro}.

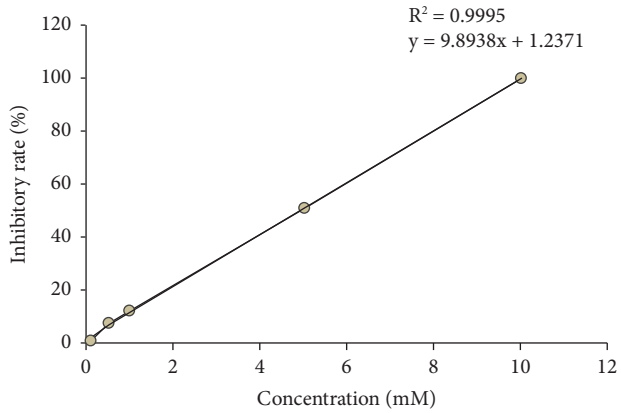

Figure 6: In vitro validation of the inhibitory activity of minocycline on M^{pro}.

Table 1: Comparison of the effect of COVID-19 and minocycline on selected biomarkers.

Biological markers	COVID-19		Minocycline effect on physical or infectious challenge	
	Severe (references)	Nonsevere (references)	In vivo (references)	In vitro (references)
ESR	↑[37–40]	↑[37, 39, 41–44]	↓[45–47]	
CRP	↑[37, 38, 48–53]	↑[37, 38, 43, 49, 50, 52, 54]	↓[47, 55–58]	
LD	↑[37, 51, 59, 60]	↑[37]		↓[51]
D-dimer	↑[37, 40, 50, 51, 59]	↑[37, 42, 43, 51, 54, 61]	↓[62]	
CD^{4+}T cell	↓[63–65]	↓[39, 64, 66]	↑[37]	
CD^{8+}T cell	↓[63, 64, 67]	↓[39, 64, 68]	↑[69]	
TNF-α	↑[63, 70]	↑[68, 71, 72]	↓[73–77]	↓[78–81]
IFN-γ	↑[63, 64]	↑[42, 64, 82]		↓[27, 80]
IL-6	↑[37, 40, 50, 63, 64, 82]	↑[37, 39, 44, 64, 66, 83]	↓[73–75, 77]	↓[80, 81, 83]
IL-10	↑[63, 64]	↑[39, 64, 68, 72]		↓[73, 78, 80, 84]

Note. ESR: erythrocyte sedimentation rate; CRP: C-reactive protein; LD: lactose dehydrogenase; TNF-α: tumor necrosis factor α; IFN-γ: interferon γ; IL-: interleukin; ↑: significantly increased; ↓: significantly decreased.

broad-spectrum biological markers especially TNF-α, IFN-γ, IL-6, and IL-10 associated with minocycline administration were opposed to those of COVID-19 condition (both severe and nonsevere), which was strongly supported by in vivo and in vitro data.

Inflammatory responses triggered by viral infection play a crucial role in pulmonary pathology severity, suppressing the IFS to reduce lung inflammation is a valuable treatment method [86]. High doses of glucocorticoid were widely applied during the outbreaks of SARS to suppress lung inflammation and immune response; however, it appeared to be associated with side effects [87–89]. Thalidomide (immunomodulatory and anti-inflammatory agent) in combination with antiviral drugs and low-dose glucocorticoid was reported the protective effect on lung injury and immunological stress caused by COVID-19 [90]. Chloroquine was included in the 6th version of Diagnostic and Treatment Protocol for COVID-19 in China due to the in vitro anti-SARS-CoV-2 results and in vivo anti-inflammatory activity. Hydroxychloroquine, which is chemically and biologically similar but safer than chloroquine, had been included in the local diagnostic and treatment guidelines for COVID-19 (Shanghai, China) [91]. In a two-year randomized controlled trial on early seropositive rheumatoid arthritis patients, minocycline achieved better anti-inflammatory outcomes than hydroxychloroquine [60]. The immune imbalance and bacterial infection often appear in the later stages of COVID-19; the efficacy of antiviral drugs might remain unsatisfactory [92]. The antibiotics and glucocorticoid were sometimes administered according to the clinical characteristics and physicians' discretion [59].

Moreover, minocycline was reported to attenuate T cell and microglia activity to impair cytokine production in T cell-microglia interaction [78]. Angiotensin converting enzyme 2 (ACE2), the function receptor for SARS-CoV-2, is present in multiple human organs [93]. Cytokine release leads to serious complications in the cardiovascular system, digestive system, and central nervous system (CNS) in COVID-19 patients [48]. Because of its high lipophilicity and small size, minocycline can cross the blood-brain barrier and accumulate in cerebrospinal fluid (CSF) and CNS cells, resulting in beneficial effects on CNS diseases.

Besides, recent evidence suggested that the precise site of interaction between minocycline and cellular RNA molecules could be double-stranded RNAs (dsRNAs), which have been observed as intermediates of the viral replication of positive-stranded viruses, the aberrant induction of inflammatory cytokines/chemokines in case of SARS infection was mostly activated by dsRNA intermediates [36, 94]. In addition, the robust viral replication and delayed IFN-γ signaling accompanying the initial steps of SARS seem to be consequence of the coronavirus ability to initially evade the host dsRNA sensors [95, 96]. Therefore, early administration of dsRNA-binding minocycline might reduce the risk of SARS-CoV-2.

4. What Is New and Conclusion

In conclusion, from in silico screening of 135 clinical drugs targeting on SARS-CoV-2 M^{pro}, minocycline, inhibitor of bacterial ribosomal rRNA, showed interesting binding affinity (−9.6 kcal/mol). Critical hydrogen bonding with the Cys145-His41 catalytic dyad and hydrophobic interactions were found between minocycline and M^{pro} active sites. During the 0–10 ns MD simulations, molecular dynamics stability of M^{pro}-minocycline complex was also demonstrated to be close to M^{pro}-N3 complex with persistent H-bond interactions. The structure-affinity relationship explained the conformational suitability of minocycline. Minocycline showed in vitro M^{pro} inhibitory activity with IC_{50} of 5 mM. Literature review found that minocycline had both in vitro and in vivo broad-spectrum antiviral as well as anti-inflammatory activities, and the levels of a broad spectrum of biological markers during minocycline administration were opposed to those of COVID-19 condition. These findings suggested that minocycline, a safe, inexpensive, and readily available antibiotic, could be considered as an adjunctive therapeutic option for severe and fast-progressive COVID-19 patients. This study shed a new light on an adjuvant treatment strategy for this viral disease. Limitations of this study include the short duration of the MD simulations, which were performed for only 10 ns, resulting in only a brief understanding of the conformational changes of M^{pro}-minocycline complex.

Data Availability

The results of in silico screening of SARS-CoV-2 M^{pro} inhibition from old drugs and the results of in silico screening of minocycline analogs used to support the findings of this study are included within the supplementary information files.

Disclosure

A previously published preprint is available at https://www.researchsquare.com/article/rs-1528733/v1 [97].

Conflicts of Interest

The authors declare that they have no conflicts of interest.

Authors' Contributions

Professors Guanhua Du and Zhanfei She conceptualized and supervised this study. Guanhua Du and Bin Xiao designed the research. Bin Xiao, Xianxiang Bai, Liwen Ren, and Jinhua Wang performed virtual screening and analyzed the docking results' analysis. Yaru Han and Si Wu designed and carried out the literature review. Yaru Han and Xiurong Luan performed the in vitro M^{pro} inhibitory assay. All authors revised the manuscript and have read and approved the final manuscript. Yaru Han, Xianxing Bai, and Su Wu contributed equally to this work.

Acknowledgments

The authors thank Professors Zihe Rao, Haitao Yang, and Xiuna Yang from Shanghai Tech University for the early donation of M^{pro} information and the preprint by the Research Square. This work was supported by the National

Natural Science Foundation of China (82260822), Central Government Funds for Guiding Local Scientific and Technological Development (2020ZY0036), Chinese Academy of Sciences "Western Light Young Scholars" grant program (2020 No. 82), Natural Science Foundation of Inner Mongolia (2022MS08034), and the Ordos Innovation Fund for Talent Team (Ordos Talent Work Leading Group 2018-No. 6, China).

Supplementary Materials

Table S1: Results of in silico screening of SARS-CoV-2 M^{pro} inhibition from old drugs. Table S2: Results of in silico screening of minocycline analogs. (*Supplementary Materials*)

References

[1] P. Xie, W. Ma, H. Tang, and D. Liu, "Severe COVID-19: a review of recent progress with a look toward the future," *Frontiers in Public Health*, vol. 8, p. 189, 2020.

[2] World Health Organization, "Emergencies disease novel coronavirus," 2019, https://www.who.int/emergencies/diseases/novel-coronavirus-2019.

[3] J. F. Demarest, M. Kienle, R. Boytz et al., "Brequinar and dipyridamole in combination exhibits synergistic antiviral activity against SARS-CoV-2 in vitro: rationale for a host-acting antiviral treatment strategy for COVID-19," *Antiviral Research*, vol. 206, Article ID 105403, 2022.

[4] J. Ziebuhr, "The coronavirus replicase," *Current Topics in Microbiology and Immunology*, vol. 287, pp. 57–94, 2005.

[5] H. Yang, W. Xie, X. Xue et al., "Design of wide-spectrum inhibitors targeting coronavirus main proteases," *PLoS Biology*, vol. 3, no. 10, p. e324, 2005.

[6] A. S. Omrani, M. M. Saad, K. Baig et al., "Ribavirin and interferon alfa-2a for severe Middle East respiratory syndrome coronavirus infection: a retrospective cohort study," *The Lancet Infectious Diseases*, vol. 14, no. 11, pp. 1090–1095, 2014.

[7] J. F. Chan, K. H. Chan, R. Y. Kao et al., "Broad-spectrum antivirals for the emerging Middle East respiratory syndrome coronavirus," *Journal of Infection*, vol. 67, no. 6, pp. 606–616, 2013.

[8] A. H. de Wilde, D. Jochmans, C. C. Posthuma et al., "Screening of an FDA-approved compound library identifies four small-molecule inhibitors of Middle East Respiratory syndrome coronavirus replication in cell culture," *Antimicrobial Agents and Chemotherapy*, vol. 58, no. 8, pp. 4875–4884, 2014.

[9] J. Dyall, C. M. Coleman, B. J. Hart et al., "Repurposing of clinically developed drugs for treatment of Middle East respiratory syndrome coronavirus infection," *Antimicrobial Agents and Chemotherapy*, vol. 58, no. 8, pp. 4885–4893, 2014.

[10] D. Nir, K. Demarco Jennifer, A. Jones Krysten et al., "Masitinib is a broad coronavirus 3CL inhibitor that blocks replication of SARS-CoV-2," *Science*, vol. 372, no. 6557, pp. 931–936, 2021.

[11] Z. Jin, X. Du, Y. Xu et al., "Structure of M^{pro} from SARS-CoV-2 and discovery of its inhibitors," *Nature*, vol. 582, no. 7811, pp. 289–293, 2020.

[12] C. A. Lipinski, F. Lombardo, B. W. Dominy, and P. J. Feeney, "Experimental and computational approaches to estimate solubility and permeability in drug discovery and development settings," *Advanced Drug Delivery Reviews*, vol. 23, no. 1-3, pp. 3–25, 1997.

[13] B. Xiao, S. Wang, Z. She et al., "Structure-based design, synthesis, PPAR-γ activation, and molecular docking of *N*-substituted phthalimides," *Medicinal Chemistry Research*, vol. 26, no. 8, pp. 1628–1634, 2017.

[14] X. Han, S. Wang, N. Zhang et al., "Novel triazole derivatives containing different ester skeleton: design, synthesis, biological evaluation and molecular docking," *Chemical and Pharmaceutical Bulletin*, vol. 68, no. 1, pp. 64–69, 2020.

[15] B. Xiao, Y. Xiao, H. Ning et al., "In vitro dual-target activities and in vivo antidiabetic effect of 3-hydroxy-N-(p-hydroxyphenethyl) phthalimide in high-fat diet and streptozotocin-induced diabetic golden hamsters," *Medicinal Chemistry Research*, vol. 29, no. 11, pp. 2077–2088, 2020.

[16] E. F. Pettersen, T. D. Goddard, C. C. Huang et al., "UCSF Chimera-a visualization system for exploratory research and analysis," *Journal of Computational Chemistry*, vol. 25, no. 13, pp. 1605–1612, 2004.

[17] F. Sanner Michel, "Python: a programming language for software integration and development," *Journal of Molecular Graphics and Modelling*, vol. 17, pp. 57–61, 1999.

[18] G. M. Morris, R. Huey, W. Lindstrom et al., "AutoDock4 and AutoDockTools4: automated docking with selective receptor flexibility," *Journal of Computational Chemistry*, vol. 30, no. 16, pp. 2785–2791, 2009.

[19] O. Trott and A. J. Olson, "AutoDock Vina: improving the speed and accuracy of docking with a new scoring function, efficient optimization, and multithreading," *Journal of Computational Chemistry*, vol. 31, no. 2, pp. 455–461, 2010.

[20] K. H. Chowdhury, M. R. Chowdhury, S. Mahmud et al., "Drug repurposing approach against novel coronavirus disease (COVID-19) through virtual screening targeting SARS-CoV-2 main protease," *Biology*, vol. 10, no. 1, p. 2, 2020.

[21] Z. Yang, "Exploring active compounds of Da-Yuan-Yin in treatment of COVID-19 based on network pharmacology and molecular docking method," *Chinese Traditional and Herbal Drugs*, vol. 51, pp. 836–844, 2020.

[22] C. U. Chukwudi, "rRNA binding sites and the molecular mechanism of action of the tetracyclines," *Antimicrobial Agents and Chemotherapy*, vol. 60, no. 8, pp. 4433–4441, 2016.

[23] J. N. Lashinsky, O. Henig, J. M. Pogue, and K. S. Kaye, "Minocycline for the treatment of multidrug and extensively drug-resistant a. baumannii: a review," *Infectious Disease and Therapy*, vol. 6, no. 2, pp. 199–211, 2017.

[24] A. D. Elmezayen, A. Al-Obaidi, A. T. Şahin, and K. Yelekçi, "Drug repurposing for coronavirus (COVID-19): in silico screening of known drugs against coronavirus 3CL hydrolase and protease enzymes," *Journal of Biomolecular Structure and Dynamics*, vol. 39, no. 8, pp. 2980–2992, 2021.

[25] R. Islam, M. R. Parves, A. S. Paul et al., "A molecular modeling approach to identify effective antiviral phytochemicals against the main protease of SARS-CoV-2," *Journal of Biomolecular Structure and Dynamics*, vol. 39, no. 9, pp. 3213–3224, 2021.

[26] S. Jakhmola, N. A. Jonniya, M. F. Sk, A. Rani, P. Kar, and H. C. Jha, "Identification of potential inhibitors against epstein–barr virus nuclear antigen 1 (EBNA1): an insight from docking and molecular dynamic simulations," *ACS Chemical Neuroscience*, vol. 12, no. 16, pp. 3060–3072, 2021.

[27] J. L. Drewes, G. L. Szeto, E. L. Engle et al., "Attenuation of pathogenic immune responses during infection with human and simian immunodeficiency virus (HIV/SIV) by the tetracycline derivative minocycline," *PLoS One*, vol. 9, no. 4, Article ID e94375, 2014.

[28] M. Michaelis, M. C. Kleinschmidt, H. W. Doerr, and J. Cinatl, "Minocycline inhibits West Nile virus replication and apoptosis in human neuronal cells," *Journal of Antimicrobial Chemotherapy*, vol. 60, no. 5, pp. 981–986, 2007.

[29] M. K. Mishra, D. Ghosh, R. Duseja, and A. Basu, "Antioxidant potential of minocycline in Japanese encephalitis virus infection in murine neuroblastoma cells: correlation with membrane fluidity and cell death," *Neurochemistry International*, vol. 54, no. 7, pp. 464–470, 2009.

[30] L. Josset, H. Zeng, S. M. Kelly, T. M. Tumpey, and M. G. Katze, "Transcriptomic characterization of the novel avian-origin influenza A (H7N9) virus: specific host response and responses intermediate between avian (H5N1 and H7N7) and human (H3N2) viruses and implications for treatment options," *mBio*, vol. 5, no. 1, pp. e01102–e01113, 2014.

[31] K. Hendricks, M. G. Parrado, and J. Bradley, "Opinion: an existing drug to assess in vivo for potential adjunctive therapy of Ebola Virus disease and post-Ebola syndrome," *Frontiers in Pharmacology*, vol. 10, p. 1691, 2019.

[32] A. Sharifi, A. Amanlou, F. Moosavi-Movahedi, S. Golestanian, and M. Amanlou, "Tetracyclines as a potential antiviral therapy against Crimean Congo hemorrhagic fever virus: docking and molecular dynamic studies," *Computational Biology and Chemistry*, vol. 70, pp. 1–6, 2017.

[33] T. Fredeking, J. Zavala-Castro, P. Gonzalez-Martinez et al., "Dengue patients treated with doxycycline showed lower mortality associated to a reduction in IL-6 and TNF levels," *Recent Patents on Anti-infective Drug Discovery*, vol. 10, no. 1, pp. 51–58, 2015.

[34] M. O. Griffin, E. Fricovsky, G. Ceballos, and F. Villarreal, "Tetracyclines: a pleitropic family of compounds with promising therapeutic properties. Review of the literature," *American Journal of Physiology: Cell Physiology*, vol. 299, no. 3, pp. C539–C548, 2010.

[35] W. Marten Norman and J. Zhou, "The role of metalloproteinases in corona virus infection," *Experimental Models of Multiple Sclerosis*, Springer, Berlin, Germany, pp. 839–848, 2005.

[36] S.-W. Ding and O. Voinnet, "Antiviral immunity directed by small RNAs," *Cell*, vol. 130, no. 3, pp. 413–426, 2007.

[37] Q. Cai, D. Huang, P. Ou et al., "COVID-19 in a designated infectious diseases hospital outside Hubei Province, China," *Allergy*, vol. 75, no. 7, pp. 1742–1752, 2020.

[38] Y. Zheng, Z. Huang, G. Yin et al., "Study of the lymphocyte change between COVID-19 and non-COVID-19 pneumonia cases suggesting other factors besides uncontrolled inflammation contributed to multi-organ injury," *medRxiv*, 2020.

[39] X. Cai, *An Insight of Comparison between COVID-19 (2019-nCoV Disease) and SARS-CoV in Pathology and Pathogenesis*, OSF Preprints, Peoria, IL, USA, 2020.

[40] X. Qi, H. Kong, W. Ding et al., "Abnormal coagulation function of patients with COVID-19 is significantly related to hypocalcemia and severe inflammation," *Frontiers of Medicine*, vol. 8, Article ID 638194, 2021.

[41] A. P. D. Iwamura, M. R. Tavares da Silva, A. L. Hümmelgen et al., "Immunity and inflammatory biomarkers in COVID-19: a systematic review," *Reviews in Medical Virology*, vol. 31, no. 4, Article ID e2199, 2021.

[42] A.-S. Hanny, L. R. S. Karp, H. Dzik Walter et al., "COVID-19 and coagulation: bleeding and thrombotic manifestations of SARS-CoV-2 infection," *Blood*, vol. 136, no. 4, pp. 489–500, 2021.

[43] M. R. Anderson, J. Geleris, D. R. Anderson et al., "Body mass index and risk for intubation or death in SARS-CoV-2 infection: a retrospective cohort study," *Annals of Internal Medicine*, vol. 173, no. 10, pp. 782–790, 2020.

[44] L. Leys, S. Donaldson, and A. Thomas, "Spontaneous pneumothorax occurring in coronavirus disease 2019 (COVID-19)," *Chest*, vol. 158, no. 4, p. 1279, 2020.

[45] B. C. Tilley, S. Alarcón Graciela, P. Heyse Stephen et al., "Minocycline in rheumatoid arthritis: a 48-week, double-blind, placebo-controlled trial," *Annals of Internal Medicine*, vol. 122, no. 2, pp. 81–89, 1995.

[46] J. R. O'Dell, K. W. Blakely, J. A. Mallek et al., "Treatment of early seropositive rheumatoid arthritis: a two-Year, double-blind comparison of minocycline and hydroxychloroquine," *Arthritis & Rheumatism*, vol. 44, no. 10, pp. 2235–2241, 2001.

[47] A. Matsuyama, N. Sakai, M. Ishigami, H. Hiraoka, and S. Yamashita, "Minocycline for the treatment of takayasu arteritis," *Annals of Internal Medicine*, vol. 143, no. 5, pp. 394-395, 2005.

[48] M. Ling, M. Wang, S. Chen et al., "Neurological manifestations of hospitalized patients with COVID-19 in wuhan, China: a retrospective case series study," *JAMA Neurology*, vol. 77, pp. 1–9, 2020.

[49] W. Cao, L. Shi, C. Lin, X. Xu, and Z. Wu, "Clinical features and laboratory inspection of novel coronavirus pneumonia (COVID-19) in Xiangyang, Hubei," *medRxiv*, 2020.

[50] L. Liu, J. Gao, W. Hu et al., "Clinical characteristics of 51 patients discharged from hospital with COVID-19 in Chongqing, China," *medRxiv*, 2020.

[51] X. Qin, S. Qiu, Y. Yuan et al., "Clinical characteristics and treatment of patients infected with COVID-19 in Shishou, China," 2020, https://ssrn.com/abstract=3541147.

[52] G. Q. Qian, N. B. Yang, F. Ding et al., "Epidemiologic and clinical characteristics of 91 hospitalized patients with COVID-19 in Zhejiang, China: a retrospective, multi-centre case series," *QJM: International Journal of Medicine*, vol. 113, no. 7, pp. 474–481, 2020.

[53] L. Xun, L. Wang, S. Yan et al., "Clinical characteristics of 25 death cases infected with COVID-19 pneumonia: a retrospective review of medical records in a single medical center, Wuhan, China," *International Journal of Infectious Diseases*, vol. 94, pp. 128–132, 2020.

[54] J. Sekhon, D. Vangipuram, K. Creed, and H. Bukamur, "ARDS related to COVID-19," *Chest*, vol. 158, no. 4, p. 2565, 2020.

[55] M. Kloppenburg, B. A. Dijkmans, C. L. Verweij, and F. C. Breedveld, "Inflammatory and immunological parameters of disease activity in rheumatoid arthritis patients treated with minocycline," *Immunopharmacology*, vol. 31, no. 2-3, pp. 163–169, 1996.

[56] K. Makoto and H. Shimizu, "A case of hypertrophic pachymeningitis treated successfully with antibiotics: the remarkable effect of minocycline hydrochloride in reducing the serum C-reactive protein value," *Neurological Surgery*, vol. 37, pp. 673–679, 2009.

[57] G. Soliman Maha, A. Hanaamansour, A. Hasan Wedad, and A. Hassaan Nahla, "Protective effect of minocycline against bacterial infection-induced sickness behavior in rats," *Global Journal of Pharmacology*, vol. 9, pp. 1–12, 2015.

[58] L. Jing, X. Wang, M. Wang, C. Wang, and G. Song, "Analyze on the influence of minocycline combined with azithromycin on serum CRP, D-Dimer and lung function in the children with refractory mycoplasma pneumonia," *Chinese Journal of Biochemical Pharmaceutics*, vol. 37, pp. 102–105, 2017.

[59] J. Dong, D. Zhang, C. Zhu et al., "Clinical characteristics predicting progression of COVID-19," 2020, https://ssrn.com/abstract=3539674.

[60] D. Wang, B. Hu, C. Hu et al., "Clinical characteristics of 138 hospitalized patients with 2019 novel coronavirus–infected pneumonia in wuhan, China," *JAMA*, vol. 323, no. 11, pp. 1061–1069, 2020.

[61] R. D. Lopes, P. G. M. de Barros e Silva, R. H. M. Furtado et al., "Therapeutic versus prophylactic anticoagulation for patients admitted to hospital with COVID-19 and elevated D-dimer concentration (ACTION): an open-label, multicentre, randomised, controlled trial," *The Lancet*, vol. 397, no. 10291, pp. 2253–2263, 2021.

[62] Y. Hou, C. H. Ryu, K. Y. Park, S. M. Kim, C. H. Jeong, and S. S. Jeun, "Effective combination of human bone marrow mesenchymal stem cells and minocycline in experimental autoimmune encephalomyelitis mice," *Stem Cell Research & Therapy*, vol. 4, p. 77, 2013.

[63] B. Diao, C. Wang, Y. Tan et al., "Reduction and functional exhaustion of T cells in patients with coronavirus disease 2019 (COVID-19)," *Frontiers in Immunology*, vol. 11, p. 827, 2020.

[64] Y. Cheng, R. Luo, K. Wang et al., "Kidney disease is associated with in-hospital death of patients with COVID-19," *Kidney International*, vol. 97, no. 5, pp. 829–838, 2020.

[65] X. Peng, J. Ouyang, I. Stéphane et al., "Sharing $CD4^+$ T cell loss: when COVID-19 and HIV collide on immune system," *Frontiers of Medicine*, pp. 11–596631, 2020.

[66] G. Schett, B. Manger, D. Simon, and R. Caporali, "COVID-19 revisiting inflammatory pathways of arthritis," *Nature Reviews Rheumatology*, vol. 16, no. 8, pp. 465–470, 2020.

[67] W. Jaana, P. Krystallenia, K. Zehra et al., "Impaired cytotoxic $CD8^+$ T cell response in elderly COVID-19 patients," *mBio*, vol. 11, no. 5, Article ID 02243, 2020.

[68] E. Delorme-Axford and D. J. Klionsky, "Highlights in the fight against COVID-19: does autophagy play a role in SARS-CoV-2 infection?" *Autophagy*, vol. 16, no. 12, pp. 2123–2127, 2020.

[69] S. Mehrotra, M. J. Pecaut, and D. S. Gridley, "Analysis of minocycline as a countermeasure against acute radiation syndrome," *In Vivo*, vol. 26, no. 5, pp. 743–758, 2012.

[70] D. M. Del Valle, S. Kim-Schulze, H. H. Huang et al., "An inflammatory cytokine signature predicts COVID-19 severity and survival," *Nature Medicine*, vol. 26, no. 10, pp. 1636–1643, 2020.

[71] E. Mortaz, P. Tabarsi, H. Jamaati et al., "Increased serum levels of soluble TNF-α receptor is associated with ICU mortality in COVID-19 patients," *Frontiers in Immunology*, vol. 12, Article ID 592727, 2021.

[72] H. Han, Q. Ma, C. Li et al., "Profiling serum cytokines in COVID-19 patients reveals IL-6 and IL-10 are disease severity predictors," *Emerging Microbes and Infections*, vol. 9, no. 1, pp. 1123–1130, 2020.

[73] A. Ledeboer, E. M. Sloane, E. D. Milligan et al., "Minocycline attenuates mechanical allodynia and proinflammatory cytokine expression in rat models of pain facilitation," *Pain*, vol. 115, no. 1, pp. 71–83, 2005.

[74] W. Masocha, M. E. Rottenberg, and K. Kristensson, "Minocycline impedes African trypanosome invasion of the brain in a murine model," *Antimicrobial Agents and Chemotherapy*, vol. 50, no. 5, pp. 1798–1804, 2006.

[75] H. Suzuki, Y. Sugimura, S. Iwama et al., "Minocycline prevents osmotic demyelination syndrome by inhibiting the activation of microglia," *Journal of the American Society of Nephrology*, vol. 21, no. 12, pp. 2090–2098, 2010.

[76] K. L. Wu, S. H. Chan, and J. Y. Chan, "Neuroinflammation and oxidative stress in rostral ventrolateral medulla contribute to neurogenic hypertension induced by systemic inflammation," *Journal of Neuroinflammation*, vol. 9, no. 1, p. 212, 2012.

[77] B. Bassett, S. Subramaniyam, Y. Fan et al., "Minocycline alleviates depression-like symptoms by rescuing decrease in neurogenesis in dorsal hippocampus via blocking microglia activation/phagocytosis," *Brain, Behavior, and Immunity*, vol. 91, pp. 519–530, 2021.

[78] F. Giuliani, W. Hader, and V. W. Yong, "Minocycline attenuates T cell and microglia activity to impair cytokine production in T cell-microglia interaction," *Journal of Leukocyte Biology*, vol. 78, no. 1, pp. 135–143, 2005.

[79] G. Szeto, A. Brice, H. Yang, S. Barber, R. Siliciano, and J. Clements, "Minocycline attenuates HIV infection and reactivation by suppressing cellular activation in human $CD4^+$ T cells," *The Journal of Infectious Diseases*, vol. 201, no. 8, pp. 1132–1140, 2010.

[80] K. Tai, H. Iwasaki, S. Ikegaya, and T. Ueda, "Minocycline modulates cytokine and chemokine production in lipopolysaccharide-stimulated THP-1 monocytic cells by inhibiting IκB kinase α/β phosphorylation," *Translational Research*, vol. 161, no. 2, pp. 99–109, 2013.

[81] H. M. Al-Kuraishy, A. I. Al-Gareeb, M. Alqarni, N. Cruz-Martins, and G. El-Saber Batiha, "Pleiotropic effects of tetracyclines in the management of COVID-19: emerging perspectives," *Frontiers in Pharmacology*, vol. 12, Article ID 642822, 2021.

[82] I. E. Galani, N. Rovina, V. Lampropoulou et al., "Untuned antiviral immunity in COVID-19 revealed by temporal type I/III interferon patterns and flu comparison," *Nature Immunology*, vol. 22, no. 1, pp. 32–40, 2021.

[83] L. Zhu, P. Yang, Y. Zhao et al., "Single-Cell sequencing of peripheral mononuclear cells reveals distinct immune response landscapes of COVID-19 and influenza patients," *Immunity*, vol. 53, no. 3, pp. 685–696.e3, 2020.

[84] L. Yang, X. Zhu, and M. O. M. Tso, "Minocycline and sulforaphane inhibited lipopolysaccharide-mediated retinal microglial activation," *Molecular Vision*, vol. 13, pp. 1083–1093, 2007.

[85] S. Wan, Q. Yi, S. Fan et al., "Characteristics of lymphocyte subsets and cytokines in peripheral blood of 123 hospitalized patients with 2019 novel coronavirus pneumonia (NCP)," *medRxiv*, 2020.

[86] J. Zheng and S. Perlman, "Immune responses in influenza a virus and human coronavirus infections: an ongoing battle between the virus and host," *Current Opinion in Virology*, vol. 28, pp. 43–52, 2018.

[87] L. J. Stockman, R. Bellamy, and P. Garner, "SARS: systematic review of treatment effects," *PLoS Medicine*, vol. 3, no. 9, p. e343, 2006.

[88] Y. M. Arabi, Y. Mandourah, F. Al-Hameed et al., "Corticosteroid therapy for critically ill patients with middle east respiratory syndrome," *American Journal of Respiratory and Critical Care Medicine*, vol. 197, no. 6, pp. 757–767, 2018.

[89] B. Venkatesh, S. Finfer, J. Cohen et al., "Adjunctive glucocorticoid therapy in patients with septic shock," *New England Journal of Medicine*, vol. 378, no. 9, pp. 797–808, 2018.

[90] Y. Li, K. Shi, F. Qi et al., "Thalidomide combined with short-term low-dose glucocorticoid therapy for the treatment of severe COVID-19: a case-series study," *International Journal of Infectious Diseases*, vol. 103, pp. 507–513, 2021.

[91] M. Wang, R. Cao, L. Zhang et al., "Remdesivir and chloroquine effectively inhibit the recently emerged novel coronavirus (2019-nCoV) in vitro," *Cell Research*, vol. 30, no. 3, pp. 269–271, 2020.

[92] C. Huang, Y. Wang, X. Li et al., "Clinical features of patients infected with 2019 novel coronavirus in Wuhan, China," *The Lancet*, vol. 395, no. 10223, pp. 497–506, 2020.

[93] Y. Zhao, Z. Zhao, Y. Wang, Y. Zhou, Y. Ma, and W. Zuo, "Single-cell RNA expression profiling of ACE2, the receptor of SARS-CoV-2," *American Journal of Respiratory and Critical Care Medicine*, vol. 202, no. 5, pp. 756–759, 2020.

[94] C. U. Chukwudi and L. Good, "Interaction of the tetracyclines with double-stranded RNAs of random base sequence: new perspectives on the target and mechanism of action," *Journal of Antibiotics*, vol. 69, no. 8, pp. 622–630, 2016.

[95] C. Y. Cheung, L. L. M. Poon, I. H. Y. Ng et al., "Cytokine responses in severe acute respiratory syndrome coronavirus-infected macrophages in vitro: possible relevance to pathogenesis," *Journal of Virology*, vol. 79, no. 12, pp. 7819–7826, 2005.

[96] X. Deng, M. Hackbart, R. C. Mettelman et al., "Coronavirus nonstructural protein 15 mediates evasion of dsRNA sensors and limits apoptosis in macrophages," *Proceedings of the National Academy of Sciences of the USA*, vol. 114, no. 21, pp. E4251–E4260, 2017.

[97] B. Xiao, S. Wu, Y. Han et al., "In silico screening of minocycline as an Mpro inhibitor and the adjunctive therapy value for the treatment of COVID-19," 2022, https://www.researchsquare.com/article/rs-1528733/v1.